第 29 卷第 12 期
2013 年 12 月

无 机 化 学 学 报
CHINESE JOURNAL OF INORGANIC CHEMISTRY

Vol.29 No.12
2688-2694

三苯基锡 9-蒽甲酸酯的合成、表征、荧光、热稳定性及量子化学研究

庾江喜[1] 邝代治*,[1] 冯泳兰[1] 张复兴[1] 王剑秋[1]
蒋伍玖[1] 朱小明[1] 彭 雁[1] 杨 溢[2]
([1]功能金属有机材料湖南省普通高等学校重点实验室,衡阳师范学院化学与材料科学系,衡阳 421008)
([2]衡阳师范学院南岳学院化学与材料科学系,衡阳 421008)

摘要: 在甲醇中三苯基氢氧化锡与 9-蒽甲酸反应,合成了有机锡配合物$[Ph_3Sn(O_2CC_{14}H_9)(MeOH)]_2\cdot MeOH$,经 IR、$^1H$ 和 ^{13}C-NMR、元素分析及 X-射线单晶衍射表征结构。晶体结构分析表明:配合物中心锡原子为五配位畸变三角双锥构型。晶体中,配合物分子的羰基氧与近邻的甲醇氧、两相邻的甲醇氧间分别形成 O–H···O 氢键,组成一维 S 形链;经链内蒽环 H 与另一蒽环的 C–H···π 作用,进一步连接成梯状结构。两相邻梯状链间,通过配位甲醇的甲基 H 与另链苯环发生 C–H···π 作用扩展成二维网状。室温下,配合物在 460 nm 处有较强的荧光发射(λ_{ex}=360 nm)。热重分析表明,配合物在 240 ℃以下能稳定存在。利用量子化学 G03W 软件,在 LANL2DZ 基组对配合物的稳定性、前沿分子轨道组成及能量进行研究。

关键词: 有机锡配合物; 晶体结构; 荧光; 热稳定性; 量子化学
中图分类号: O614.43+2 **文献标识码**: A **文章编号**: 1001-4861(2013)12-2688-07
DOI:10.3969/j.issn.1001-4861.2013.00.373

Synthesis, Characterization, Fluorescence, Thermal Property and Quantum Chemistry of Triphenyltin 9-Anthroicarboxylate

YU Jiang-Xi[1] KUANG Dai-Zhi*,[1] FENG Yong-Lan[1] ZHANG Fu-Xing[1]
WANG Jian-Qiu[1] JIANG Wu-Jiu[1] ZHU Xiao-Ming[1] PENG Yan[1] YANG Yi[2]
([1]*Key Laboratory of Functional Organometallic Materials of College of Hunan Province, Department of Chemistry and Material Science, Hengyang Normal University, Hengyang, Hunan* 421008, *China*)
([2]*Department of Chemistry and Material Science, Hengyang Normal University Nanyue College, Hengyang, Hunan* 421008, *China*)

Abstract: A new organotin complex $[Ph_3Sn(O_2CC_{14}H_9)(CH_3OH)]_2\cdot CH_3OH$ has been synthesized by the reaction of triphenyltin hydroxide with 9-anthroic acid in methanol. It was characterized by IR, ^1H and ^{13}C NMR, elemental analysis and X-ray crystal diffraction. Crystal structure shows a distorted trigonal bipyramidal configuration with five-coordination for the central tin atom. In the crystal, O–H···O hydrogen-bond interactions exist between the methanol O atom and the carbonyl O atom in an adjacent complex molecule, and between the neighboring methanol O atoms, resulting in the formation of a 1D S-shaped chain. Due to the C–H···π interactions between anthryl-H and anthracene ring, the obtained chain is further linked to form 1D ladderlike structure. Finally, a 2D network has been generated by the C–H···π interactions between methyl-H and benzene ring in the neighbouring 1D ladderlike chains. Fluorescence spectra of the complex reveals a strong emission band at 460 nm when excited with 360 nm radiation at room temperature. Thermogravimetric analysis shows that the complex is stable

收稿日期:2013-02-13。收修改稿日期:2013-07-03。
湖南省自然科学基金(No.11JJ3021),湖南省科技计划(No.2013TZ2025)湖南省教育厅创新平台开放基金(No.10K010)和一般项目(No.12C0537),湖南省普通高校功能金属有机材料重点实验室开放基金(No.10K02),衡阳市科技计划(No.2011KG56,2012KJ30),衡阳师范学院青年骨干教师培养计划(2012)及南岳学院大学生研究性学习与创新性实验(No.NYD201205)资助项目。
*通讯联系人。E-mail:hnkdz@qq.com;会员登记号:S06N8374M1012。

up to 240 ℃. The stability of the complex, the orbital energies and composition characteristics of some frontier molecular orbitals have been investigated at LANL2DZ level with G03W software. CCDC: 899826.

Key words: organotin complex; crystal structure; fluorescence; thermal stability; quantum chemistry

0 Introduction

Organotin complexes have attracted great interest due to their remarkable structural diversity[1], potential therapeutic activities[2], industrial and agricultural applications[3]. They have extensive application prospects, such as biocides[4], catalysts[5], stabilizers[6] and wood preservatives[7]. In recent years, they have also been investigated as anti-tumor[8] and anti-tuberculosis agents[9]. Moreover, they have shown anti-fouling[10], anti-inflammatory [11] and anti-microbial activities[12] as well. However, only a few reports regarding organotin complexes as electroactive[13-14] and photoactive[15] materials during the past decade, which is precisely what we are interested in. To continue our interest in this field, we chose 9-anthroic acid as ligand, and we have obtained a new organotin complex by means of this ligand with triphenyltin hydroxide. Herein we report the synthesis and characterization of the complex.

1 Experimental

1.1 Materials and measurements

All reagents were of analytical grade obtained from commercial sources and used without further purification. The melting point was obtained on an X-4 microscopic melting point apparatus and is uncorrected. IR spectra (KBr pellet) was recorded on a Shimadzu IRPrestige-21 spectrometer (4 000~400 cm^{-1} range). ^1H and ^{13}C NMR spectra were measured at 400.13 and 100.62 MHz, respectively, in $CDCl_3$ on a Bruker Avance 400 spectrometer using TMS as internal standard. Elemental analysis of C, H was performed with a Perkin-Elmer 2400 Ⅱ elemental analyser. Fluorescence (FL) emission spectra were measured using a HITACHI F-7000 fluorescence spectrophotometer. Thermal stability was measured on a Netzsch TG 209 F3 thermogravimetric analyzer at a heating rate of 20 ℃·min^{-1} under N_2 atmosphere.

1.2 Synthesis

A mixture of Ph_3SnOH (0.367 g, 1 mmol), 9-anthroic acid (0.222 g, 1 mmol) and CH_3OH (20 ml) was stirred and heated at reflux for 1 h. After cooling down to room temperature, the solution was filtered. Straw yellow crystals were obtained by the slow evaporation of methanol solution at room temperature after a week. Yield: 0.561 g (90.6%). M.p. 138~140 ℃. Anal. Calcd. for $C_{69}H_{60}O_7Sn_2$: C, 66.91; H, 4.88. Found: C, 66.89; H, 4.83. IR (cm^{-1}): 3 377.5 (b, ν_{O-H}); 3 049.6 (w, ν_{Ar-H}); 1 525.8 (s, $\nu_{as}COO$); 1 320.3 (m, ν_sCOO); 556.5 (w, ν_{Sn-C}); 459.1 (w, ν_{Sn-O}). ^1H NMR (ppm): 8.46 (s, 1H, 10-anthracene-H), 7.85~8.03 (m, 8H, 1~8-anthracene-H), 7.35~7.51 (m, 15H, Ph-H). ^{13}C NMR (ppm): 125.30, 125.75, 126.62, 128.47, 128.54, 128.81, 129.14, 129.46, 130.43, 131.18, 136.93, 137.17, 137.41, 138.32 (Ar-C), 176.06 (COO).

1.3 Determination of crystal structure

X-ray diffraction data for the crystal was performed with graphite monochromated Mo *Ka* radiation (λ=0.071 073 nm) on a Bruker Smart Apex Ⅱ CCD diffractometer, and collected by the φ-ω scan technique at 296(2) K. Multi-scan absorption correction was applied to the data. The crystal structure was solved by direct methods and refined by full-matrix least-squares on F^2. All the non-hydrogen atoms were located in successive difference Fourier syntheses and then refined anisotropically. H3A and H6A were located in successive difference Fourier syntheses, but the other hydrogen atoms were placed in calculated positions, and then all of which were refined isotropically with the isotropic vibration parameters related to the parent atom. All calculations were performed with SHELXTL-97 programs[16]. Fig.1 and Fig.2 were obtained from the DIAMOND 3.1c software package. The crystal data and structure refinement parameters of this complex are listed in Table 1.

Table 1 Crystal data and structure refinement parameters of the complex

Empirical formula	$C_{69}H_{60}O_7Sn_2$	Absorption coefficient / mm^{-1}	0.892
Formula weight	1 238.55	$F(000)$	2 520
Temperature / K	296(2)	Crystal size / mm	0.21×0.17×0.13
Wavelength / nm	0.071 073	θ range for data collection / (°)	2.22 to 25.05
Crystal system	Monoclinic	Limiting indices	$-12 \leqslant h \leqslant 11, -32 \leqslant k \leqslant 36, -22 \leqslant l \leqslant 23$
Space group	$P2_1/c$	Reflections collected / unique	33 465 / 10 502 (R_{int}=0.028 3)
a / nm	1.014 84(4)	Completeness to θ / %	99.7
b / nm	3.054 41(14)	Data / restraints / parameters	10 502 / 222 / 685
c / nm	1.933 89(7)	Goodness-of-fit on F^2	1.156
β / (°)	96.880(2)	Final R indices ($I>2\sigma(I)$)	R_1=0.046 4, wR_2=0.128 2
Volume / nm^3	5.951 4(4)	R indices (all data)	R_1=0.060 4, wR_2=0.136 5
Z	4	Largest diff. peak and hole / ($e \cdot nm^{-3}$)	748 and −503
D_c / ($g \cdot cm^{-3}$)	1.382		

CCDC: 899826.

1.4 Quantum chemistry calculation

According to the method described in reference[17], quantum chemistry calculation of the complex was performed with Gaussian03W program at B3LYP/LANL2DZ level on a P4 personal computer. For modeling the initial guess of title complex was obtained from the X-ray refinement data. In order to save time, a complex molecule was used in the calculation. The frontier molecular orbital surfaces are visualized by GaussView Molecular Visualization program.

2 Results and discussion

2.1 IR and NMR spectra

The absorption frequencies of interest are ν(COO), ν(Sn-C) and ν(Sn-O). The absence of a broad band in the range 3 100~2 500 cm^{-1} appearing in the ligand acid, as ν(OH) vibrations, indicating metal-ligand bond formation through this site. Similarly, weak absorption appear at 556.5 and 459.1 cm^{-1}, assigned to Sn-C and Sn-O bonds, respectively, also support the formation of complex[18]. The shift in ν(COO) vibrations to lower frequencies as compare to ligand acid and magnitude of $\Delta\nu$(COO) (205.5 cm^{-1}) indicating a monodentate nature of the carboxylate towards the Sn atom[19]. This assumption is consistent with the result of X-ray diffraction.

The ^{1}H NMR spectra of the complex exhibits multi signals at 7.35~8.46 corresponding to the aromatic protons. In the ^{13}C NMR spectra, the chemical shifts of the carboxylic carbon are observed at 176.06 ppm, while the aromatic carbons give signals in the range 125.30~138.32.

2.2 Description of the structure

The asymmetric unit of the complex is shown in Fig.1, Selected bond lengths and angles are given in Table 2. The asymmetric unit of the complex contains two independent complex molecules and one free methanol molecule. As we can see, the two complex molecules show similar structures, each of the two tin atoms has a coordination number of five and is surrounded by three phenyl groups, one methanolic O and one carboxylate O atom in a trigonal-bipyramidal geometry. Three Ph-C atoms are in the equatorial plane (C1, C7 and C13 for Sn1; C35, C41 and C47 for Sn2), the sums of the C-Sn-C angles are not 360°

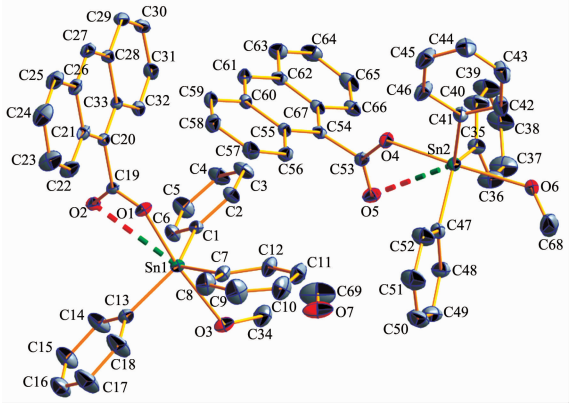

Hydrogen atoms are omitted for clarity

Fig.1 Asymmetric unit of the complex with 15% probability ellipsoids

Table 2　Selected bond lengths (nm) and angles (°) for the complex

Sn1-C1	0.210 6(4)	Sn1-C7	0.212 7(5)	Sn1-C13	0.211 2(6)
Sn1-O1	0.213 74(17)	Sn1-O3	0.248 0(3)	Sn2-C35	0.210 3(5)
Sn2-C41	0.213 7(5)	Sn2-C47	0.210 9(5)	Sn2-O4	0.214 3(4)
Sn2-O6	0.241 92(18)	Sn1…O2	0.314 9	Sn2…O5	0.317 3
C1-Sn1-C7	120.7(2)	C1-Sn1-C13	121.71(18)	C7-Sn1-C13	114.2(2)
O1-Sn1-C1	93.98(14)	O1-Sn1-C7	92.47(15)	O1-Sn1-C13	102.13(17)
O3-Sn1-C1	81.17(16)	O3-Sn1-C7	86.11(17)	O3-Sn1-C13	84.39(19)
O1-Sn1-O3	173.31(11)	C35-Sn2-C41	118.4(2)	C35-Sn2-C47	126.83(19)
C41-Sn2-C47	113.4(2)	O4-Sn2-C35	93.4(2)	O4-Sn2-C41	89.59(18)
O4-Sn2-C47	98.30(19)	O6-Sn2-C35	83.92(18)	O6-Sn2-C41	90.06(16)
O6-Sn2-C47	84.84(16)	O4-Sn2-O6	176.71(12)		

but 356.61° for Sn1, 358.63° for Sn2, so that the Sn atom and the three Ph-C atoms bonded to which are not contained in the same plane. The two O atoms occupy the apical positions (O1 and O3 for Sn1, O4 and O6 for Sn2), the axial O-Sn-O angles are not 180° but 173.31° for O1-Sn1-O3, 176.71° for O4-Sn2-O6, it proves the distortion of the geometry. The Sn-C bond lengths lie in the range of 0.210 3~0.213 7 nm, which are consistent with those reported in other triphenyltin(Ⅳ) complexes[20]. The Sn-O (methanolic oxygen atom) (O3 for Sn1; O6 for Sn2) bond lengths are 0.248 0 and 0.241 92 nm, respectively, which are slightly longer than the Sn-O covalent bond length (0.216 nm)[21] but considerably shorter than the sum of the van der Waals radii of the two atoms (0.368 nm)[22]. It indicates that the methanolic oxygen atom and tin atom form a stable intermolecular coordinative bond. The Sn-O (oxygen atom of carboxylate ligand) (O1 for Sn1; O4 for Sn2) bond lengths are 0.21374, 0.2143 nm, which shows that the carboxylate O atom is coordinated to the tin atom by a strong chemical bond. However, the carbonyl O atoms have weak interactions with Sn (O2 for Sn1; O5 for Sn2): Sn1…O2 0.314 9 nm, Sn2…O5 0.317 3 nm. If this weak interaction is taken into account, the geometry of tin atoms is best described as distorted octahedron.

As shown in Table 3, in the crystal, O−H…O hydrogen-bond interactions exist between the methanol O atom and the carbonyl O atom in an adjacent complex molecule, and between the neighboring methanol O atoms, resulting in the formation of a 1D S-shaped chain. Due to the C−H…π interactions ($d_{C29-H29\cdots Cg(A)}$=0.298 96 nm, ∠C29−H29…Cg(A)=123.275°, Cg(A) (Centroid: 0.029 60, 0.530 08, −0.140 55) is the anthracene ring composing of C54^{iv}, C55^{iv}, C56^{iv}, C57^{iv}, C58^{iv}, C59^{iv}, C60^{iv}, C61^{iv}, C62^{iv}, C63^{iv}, C64^{iv}, C65^{iv}, C66^{iv} and C67^{iv}, ^{iv} $-x$, $1-y$, $-z$) between anthryl-H and anthracene ring, the obtained chain is further linked to form 1D ladderlike structure (Fig.2a). Finally, a 2D network (Fig.2b) has been generated by the C−H…π interactions ($d_{C34-H34A\cdots Cg(B)}$= 0.346 45 nm, ∠C34−H34A…Cg(B)=147.327°, Cg(B) (Centroid: −0.305 25, 0.482 32, 0.620 57) is the benzene ring composing of C7^{v}, C8^{v}, C9^{v}, C10^{v}, C11^{v} and C12^{v}, ^{v} $-x$, $1-y$, $1-z$) between methyl-H and benzene ring in the neighbouring 1D ladderlike chains.

Table 3　Distances and angles of hydrogen bonding for the complex

D−H…A	d(D-H) / nm	d(H…A) / nm	d(D…A) / nm	∠DHA / (°)
O3−H3A…O7^{i}	0.081 98	0.186 76	0.266 43	163.673
O7^{i}−H7A^{i}…O5^{ii}	0.082 00	0.185 78	0.267 07	170.980
O6^{iii}−H6A^{iii}…O2	0.081 92	0.189 85	0.269 19	162.780

Symmetry codes: ^{i} $1-x$, $1-y$, $1-z$; ^{ii} $-x$, $1-y$, $1-z$; ^{iii} $-x$, $1/2+y$, $1/2-z$.

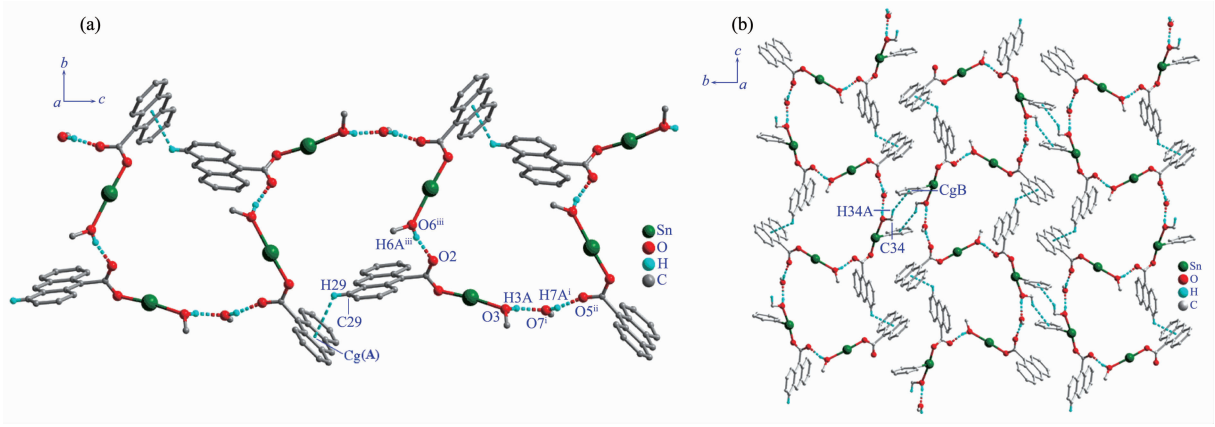

Some phenyl groups are omitted for clarity

Fig.2 (a) 1D ladderlike structure of the complex by O–H···O and C–H···π interactions; (b) 2D supramolecular structure of the complex by O–H···O and C–H···π interactions

2.3 Fluorescence Property

Fluorescence behaviours of the ligand and complex have been studied at room temperature with sample concentration of 1.0×10^{-4} mol·L^{-1} in methanol. The results show the emission spectrum of the complex is a broad band peaking at 460 nm with the excitation wavelength of 360 nm, which is similar to that of the ligand excited at 340 nm. This could be due to intraligand π-π* transitions. As shown in Fig. 3, Remarkable enhancement in fluorescence intensity was observed in the complex. The reason may be that the electron-attractive ability of carboxyl group is reduced after complexation with triphenyltin.

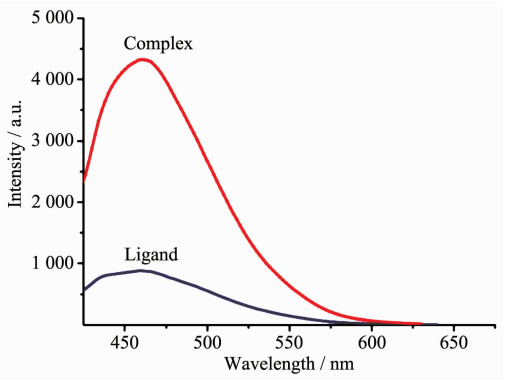

Fig.3 Emission spectra of the complex and ligand

2.4 Thermal analysis

Thermogravimetric analyse was carried out for the complex, in order to investigate its thermal stability (Fig.4). The thermogravimetric curve shows that the complex is stable up to 240 ℃, and then a noticeable weight loss up to 445 ℃ is seen (nearly 79.4%). After this, no weight loss occurs. Assuming that the residue corresponds to SnO_2, the observed weight of residue is basically in agreement with the calculated value (Calcd. 24.3%). Thus, the organotin complex described herein show good thermal stability.

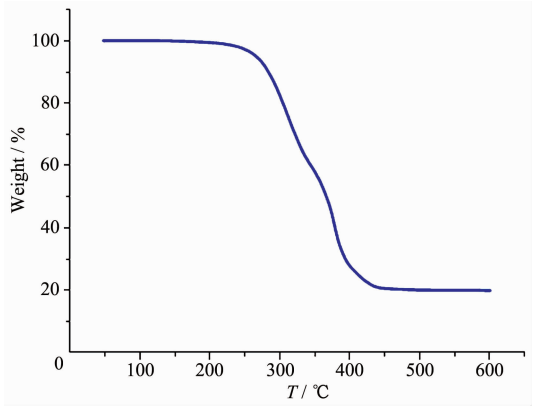

Fig.4 Thermogravimetric analysis curve of the complex

2.5 Quantum chemistry study

The calculation covered 66 atoms, 397 basis functions, 1 049 primitive gaussians, 130 alpha electrons and 130 beta electrons. For this complex, the total molecular energy is −1 540.677 418 56 a.u., the energies of HOMO and LUMO are −0.179 87 and −0.045 07 a.u., respectively. The $\Delta E(E_{LUMO}-E_{HOMO})$ value is 0.134 8 a.u., which shows the title complex is stable in the ground state.

In order to explore the bonding characteristics of the complex, the molecular orbitals were investigated systematically. The sum of the square of atomic

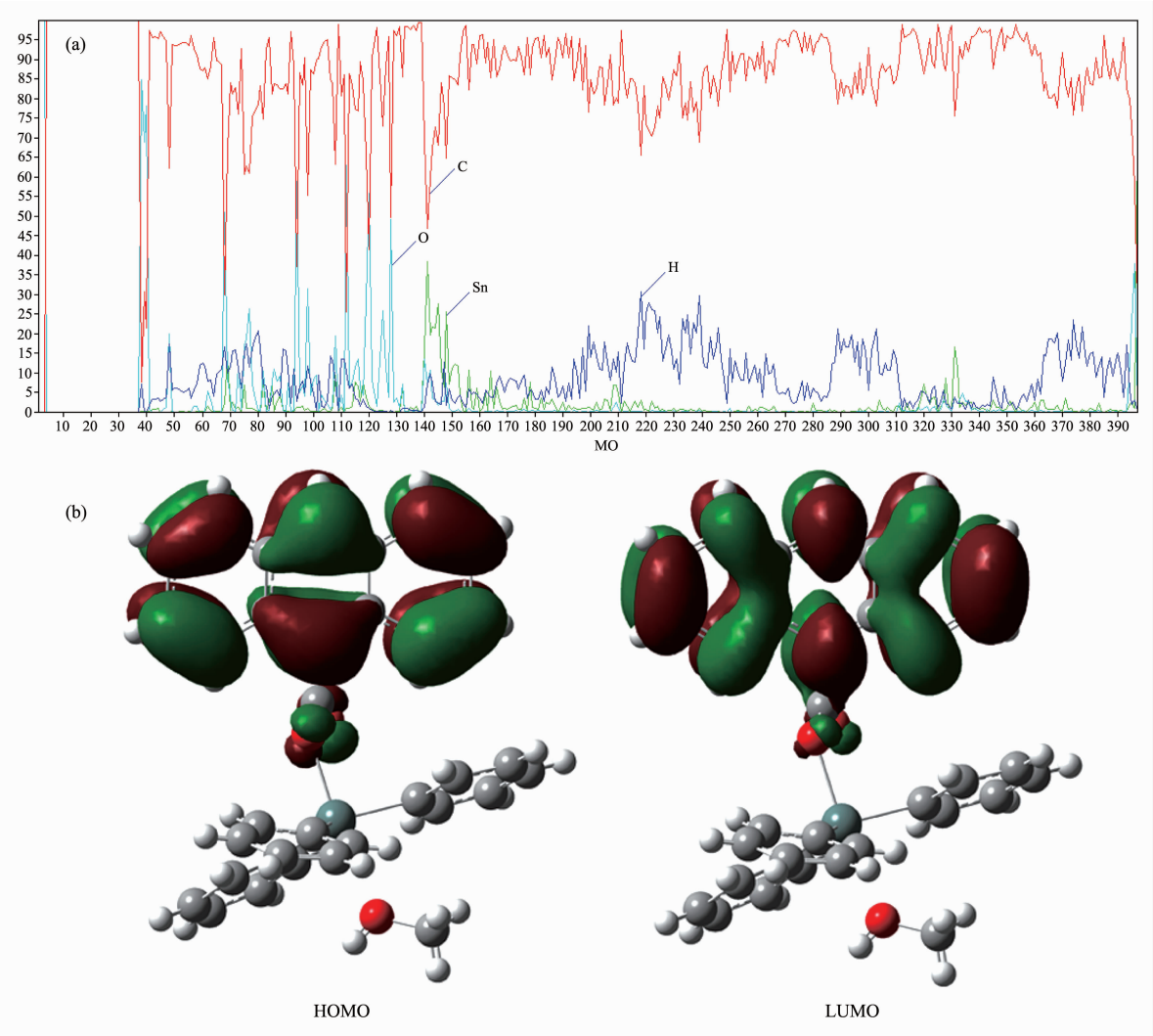

Fig.5　(a) Molecular orbitals composition of the complex at LANL2DZ level; (b) Schematic diagram of frontier MO for the complex

Table 4　Calculated some frontier molecular orbitals composition (%) of the complex at LanL2DZ level

MO	*E* / a.u.	Sn	O	C	H
130_{HOMO}	−0.179 87	0.18	3.65	96.10	0.04
131_{LUMO}	−0.045 07	0.35	1.23	98.37	0.04

orbital coefficient was used to represent the contribution of each type of atom to molecular orbital and normalized. The atoms of the complex were divided into four groups (Sn; O; C; H).

Molecular orbitals composition of the complex is shown in Fig.5a, the frontier molecular orbitals component of the complex is shown in Fig.5b, the contribution of C, H, O and Sn atoms to HOMO and LUMO are listed in Table 4. We can see that the HOMO is composed chiefly of O and C atoms, and so is the LUMO. Certainly when electron transfer occurs from ground state to excited state, electrons mainly transfer from the carboxyl O atoms to the anthryl C atoms to generate a charge transfer complex.

References:

[1] Chandrasekhar V, Gopal K, Thilagar P. *Acc. Chem. Res.*, **2007**,**40**(6):420-434

[2] TIAN Lai-Jin(田来进), YANG Hong-Jun(杨红军), ZHENG Xiao-Liang(郑晓亮), et al. *Chinese J. Inorg. Chem.*(*Wuji Huaxue Xuebao*), **2009**,**25**(7):1205-1211

[3] Davies A G, Gielen M, Pannell K H, et al. *Tin Chemistry*. Chichester: John Wiley & Sons, **2008**:431,667

[4] CAO Zuo-Ying(曹佐英), XU Hai-Feng(许海峰), TANG Rui-Ren(唐瑞仁), et al. *Chinese J. Inorg. Chem.*(*Wuji Huaxue Xuebao*), **2008**,**24**(3):474-478

[5] DU Zhi-Ping(杜治平), LIU Liang(刘亮), WANG Gong-Ying(王公应), et al. *Chinese J. Inorg. Chem.*(*Wuji Huaxue Xuebao*), **2009**,**25**(12):2225-2228

[6] Suzuki T, Takakura I, Yoda M. *Eur. Polym. J.*, **1971**,**7**(8):1105-1110

[7] Davies A G. *Organotin Chemistry*. Weinheim: Wiley-VCH Verlag GmbH & Co. KGaA, **2004**:383

[8] TIAN Lai-Jin(田来进), SUN Yu-Xi(孙玉希), ZHENG Xiao-Liang(郑晓亮), et al. *Chinese J. Inorg. Chem.*(*Wuji Huaxue Xuebao*), **2006**,**22**(4):629-632

[9] Kovala-Demertzi D, Dokorou V, Primikiri A, et al. *J. Inorg. Biochem.*, **2009**,**103**(5):738-744

[10]Lecat J L, Devaud M. *J. Organomet. Chem.*, **1983**,**244**(3):217-224

[11]Kovala-Demertzi D. *J. Organomet. Chem.*, **2006**,**691**(8):1767-1774

[12]WANG Zhi-Hong(王志宏), WANG He(王贺), GUO Yan-Zhao(郭彦召), et al. *Chinese J. Inorg. Chem.*(*Wuji Huaxue Xuebao*), **2012**,**28**(9):1926-1934

[13]YU Jiang-Xi(庾江喜), KUANG Dai-Zhi(邝代治), YIN Du-Lin(尹笃林), et al. *Chinese J. Inorg. Chem.*(*Wuji Huaxue Xuebao*), **2010**,**26**(8):1507-1510

[14]KUANG Dai-Zhi(邝代治), YU Jiang-Xi(庾江喜), YIN Du-Lin(尹笃林), et al. *Chinese J. Inorg. Chem.*(*Wuji Huaxue Xuebao*), **2010**,**26**(12):2303-2306

[15]Chandrasekhar V, Thilagar P, Steiner A, et al. *Chem.-Eur. J.*, **2006**,**12**(34):8847-8861

[16]George M S. *SHELXTL*-97: *Program for Crystal Structure Analysis*. Göttingen: University of Göttingen, **1997**.

[17]KUANG Dai-Zhi(邝代治), CHEN Zhi-Min(陈志敏), ZHANG Fu-Xing(张复兴), et al. *Chinese J. Inorg. Chem.*(*Wuji Huaxue Xuebao*), **2006**,**22**(11):1947-1951

[18]KE Yi-Kan(柯以侃), DONG Hui-Ru(董慧茹). *Analysis Chemistry handbook*, *Vol.*3(分析化学手册:第三分册). Beijing: Chemical Industry Press, **1998**:932,935

[19]XIE Qing-Lan(谢庆兰), XU Xiao-Hua(徐效华), ZHANG Dian-Kun(张殿坤), et al. *Acta Chimica Sinica*(*Huaxue Xuebao*), **1992**,**50**(5):508-514

[20]Geng W Q, Zhou H P, Cheng L H, et al. *Polyhedron*, **2012**,**31**(1):738-747

[21]Alcock N W, Timms R E. *J. Chem. Soc. A*, **1968**:1873-1876

[22]Bondi A. *J. Phys. Chem.*, **1964**,**68**(3):441-451